ERDC/CRREL TR-22-8

US Army Corps
of Engineers®
Engineer Research and
Development Center

ERDC
ENGINEER RESEARCH & DEVELOPMENT CENTER

Engineering for Polar Operations, Logistics, and Research (EPOLAR)

SAGE-PEDD Theory Manual

Modeling Windblown Snow Deposition around Buildings

Robert B. Haehnel, Yonghu Wenren, and Luke D. Allen

August 2022

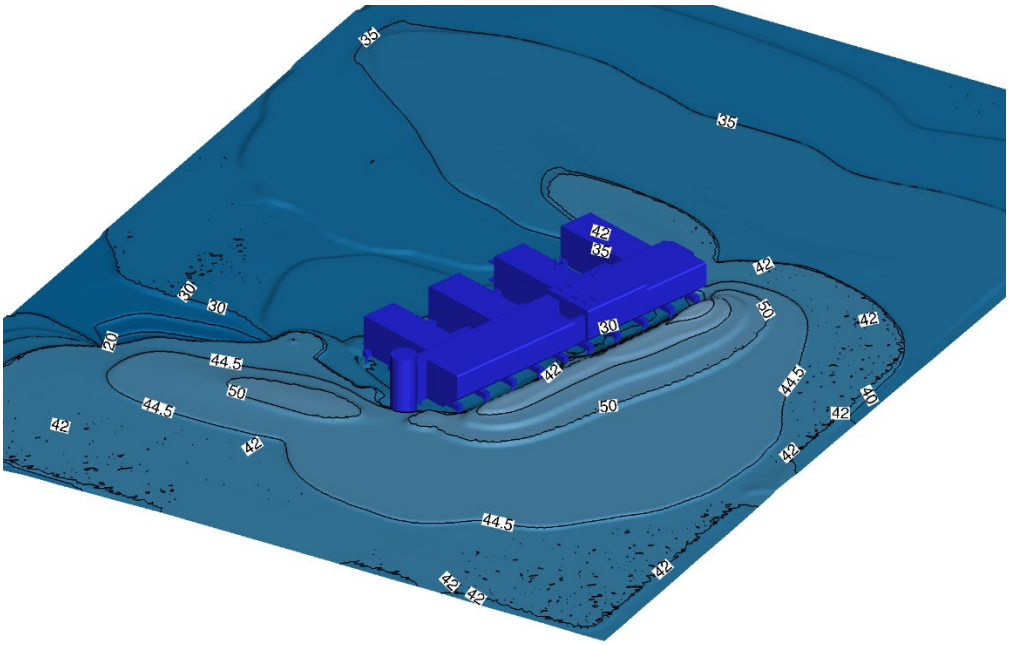

Cold Regions Research
and Engineering Laboratory

The US Army Engineer Research and Development Center (ERDC) solves the nation's toughest engineering and environmental challenges. ERDC develops innovative solutions in civil and military engineering, geospatial sciences, water resources, and environmental sciences for the Army, the Department of Defense, civilian agencies, and our nation's public good. Find out more at www.erdc.usace.army.mil.

To search for other technical reports published by ERDC, visit the ERDC online library at https://erdclibrary.on.worldcat.org/discovery.

ERDC/CRREL TR-22-8
August 2022

SAGE-PEDD Theory Manual

Modeling Windblown Snow Deposition around Buildings

Robert B. Haehnel, Yonghu Wenren, and Luke D. Allen

US Army Engineer Research and Development Center (ERDC)
Cold Regions Research and Engineering Laboratory (CRREL)
72 Lyme Road
Hanover, NH 03755-1290

Final Report

Prepared for National Science Foundation
Office of Polar Programs
Antarctic Infrastructure and Logistics
2415 Eisenhower Avenue
Alexandria, VA 22314

Under Engineering for Polar Operations, Logistics, and Research (EPOLAR)
ANT-21-54, “Impact of Lifting the Elevated South Pole Station on Snow Drift Accumulation on Nearby Facilities”

Abstract

Numerical modeling of snowdrifting is a useful tool for assessing the impact of building design on operations and facility maintenance. Here we outline the theory for the SAGE-PEDD snowdrift model that has application for determining snowdrift accumulation around buildings. This model uses the SAGE computational fluid dynamics code to determine the flow field in the computational domain. A particle entrainment, dispersion, and deposition (PEDD) model is coupled to SAGE to simulate the movement and deposition of the snow within the computational domain. The report also outlines areas of future development that upgrades to the SAGE-PEDD model should address.

Contents

Abstract ii

Contents iii

Figures and Tables iv

Preface v

1 Introduction 1

1.1 Background 1
1.2 Objectives 1
1.3 Approach 1

2 Theory 2

2.1 SAGE 2
2.1.1 Vorticity confinement 2
2.1.2 Field and surface confinement 4
2.2 Particle entrainment, dispersion, and deposition (PEDD) 5
2.2.1 Snow depth 9
2.2.2 Scaling time 9
2.2.3 Domain boundary conditions 11
2.2.4 Particle drag effects 13
2.2.5 Snow aging/sintering 13

3 Summary and future work 16

References 17

Report Documentation Page 19

Figures

1. Concentration profile measurements for varying wind speeds. Dotted lines indicate fitted curves. 12
2. Plot of fitting parameter, *A*, versus wind speed. 12
3. Flow chart detailing the snow-hardening decision tree, where $\boldsymbol{\Delta\zeta/\Delta t}$ is the change in snow depth for the current time step, $\boldsymbol{u10}$ is the wind speed at a reference height of 10 m, and $\boldsymbol{u*t,max}$ is the maximum friction velocity generated by naturally occurring winds (generally, $\boldsymbol{u*t,max}$ = 1.7 m/s, corresponding to $\boldsymbol{u10}$ = 40 m/s). 14

Preface

This study was conducted for the National Science Foundation (NSF), Office of Polar Programs, Antarctic Infrastructure and Logistics, under Engineering for Polar Operations, Logistics, and Research (EPOLAR) ANT-21-54, "Impact of Lifting the Elevated South Pole Station on Snow Drift Accumulation on Nearby Facilities." The technical monitor was Mr. Michael Gencarelli, NSF.

The work was performed by the Terrestrial and Cryospheric Sciences Branch (Dr. John Weatherly, chief) and the Engineering Resources Branch (Dr. Melisa Nallar, acting chief) of the Research and Engineering Division, US Army Engineer Research and Development Center (ERDC), Cold Regions Research and Engineering Laboratory (CRREL). At the time of publication, Dr. Caitlin A. Callaghan was division chief, and Dr. Rosa Affleck was the EPOLAR program manager. The acting deputy director of ERDC-CRREL was Mr. Bryan E. Baker, and the director was Dr. Joseph L. Corriveau.

The cover image shows simulated results of snowdrifts deposited around the elevated-building at the Amundsen-Scott South Pole Station. The image was reproduced from A. Allen, R. Haehnel, and Y. Wenren, *South Pole Station Snowdrift Model*, ERDC/CRREL TR-22-7 (Hanover, NH: US Army Engineer Research and Development Center, Cold Regions Research and Engineering Laboratory, 2022), http://dx.doi.org/10.21079/11681/44943, public domain. Portions of Section 2.2 have been modified and reprinted from C. C. Ryerson, R. B. Haehnel, G. G. Koenig, and M. M. Moulton, "Visibility Enhancement in Rotorwash Clouds," in *Proceedings of the 43rd AIAA Aerospace Sciences Meeting and Exhibit*, 10–13 January, Reno, NV (2005), https://doi.org/10.2514/6.2005-263, public domain.

COL Christian Patterson was commander of ERDC, and Dr. David W. Pittman was the director.

This page intentionally left blank.

1 Introduction

1.1 Background

This report details the underlying methods used for a computational model for predicting snowdrift development around buildings and encampments. This is intended as a tool for building design and site planning to evaluate the effects of changes in building design and site layout on drift location and volume.

1.2 Objectives

In this report we provide the theoretical basis (section 2) for the SAGE-PEDD model used to simulate snowdrift deposition around buildings. In section 3 we outline the limitations of the current model and future work needed to address these shortcomings.

1.3 Approach

The starting point for the model uses the SAGE flow solver (Wenren, Steinhoff, and Caradonna 2005; Steinhoff and Wenren 2006) coupled with a particle entrainment and dispersion (PED) model (Haehnel et al. 2008). SAGE is a general-purpose flow solver developed by the University of Tennessee Space Institute and Flow Analysis, Inc. We selected it due to our extensive experience using SAGE for rotorcraft analysis applications (Steinhoff and Wenren 2006; Wenren, Steinhoff, and Caradonna 2005) as well as related prior work incorporating the PED model (Haehnel et al. 2008). An additional advantage of SAGE is its use of the Euler equations over the more general Navier-Stokes equations, improving the computationally efficiency. Furthermore, SAGE employs the vorticity confinement method, a computationally efficient method to preserve vorticial flow structure over long times, preserving the complicated, time-varying flow structures that drive particle entrainment and dispersion. The previous work of Haehnel et al. (2008) did not consider deposition and accumulation of the particles on the ground after they were lifted into the air. This deposition aspect is necessary to model snowdrift accumulation. In this work, we added to the PED model a deposition (D) component to simulate the snowdrift deposition that occurs due to wind events; with this added component, the result is what we call SAGE-PEDD. The next section describes the theoretical background for SAGE-PEDD.

2 Theory

2.1 SAGE

The University of Tennessee Space Institute and Flow Analysis Inc. developed SAGE (Wenren et al. 2006) as an unsteady-flow solver of the Euler equations on uniform structured grids. SAGE uses the vorticity confinement (VC) method to efficiently capture over about two grid cells the vortices and the boundary-layer flow for objects immersed in the grid.

2.1.1 Vorticity confinement

The VC method solves the system of equations, representing the unsteady inviscid, incompressible mass and momentum continuity equations:

Mass:

$$\nabla \cdot \vec{V} = 0. \tag{1}$$

Momentum:

$$\frac{\partial \vec{V}}{\partial t} + \left(\vec{V} \cdot \nabla\right)\vec{V} = \frac{1}{\rho}\nabla P + \vec{\Psi}, \tag{2}$$

where

$\vec{V}$ = the fluid velocity field,
ρ = the fluid density,
P = the pressure field, and
t = time.

$\vec{\Psi}$ is a source term added to the momentum equation to affect VC:

$$\vec{\Psi} = \mu_d \nabla^2 \vec{V} - \varepsilon \hat{n} \times \hat{\omega}, \tag{3}$$

where

$\hat{\omega}$ = the local vorticity vector,
$\hat{n}$ = a unit vector defining the local direction of confinement (discussed later),
μ_d = the diffusion coefficient, and

ε = the confinement coefficient.

The first term of $\overrightarrow{\Psi}$ is a diffusive operator; the second is the VC operator. The diffusive operator acts as a counterbalance to the confinement term so that a local, thin equilibrium vortical structure results.

The flow field is adapted using a fractional-time-step approach as follows. First, the terms in the momentum equation are individually inserted as the right-hand side of an explicit time-stepping equation. Advancement from $t = n$ to $t = n + 1$ is accomplished by applying the convection term to the time derivative. In discretized form,

$$\vec{V}' = \vec{V}^n - \Delta t\left(\vec{V} \cdot \nabla\right)\vec{V}^n. \tag{4}$$

The fractional step involves updating the flow field with the confinement term:

$$\vec{V}'' = \vec{V}' - \Delta t\overrightarrow{\Psi}'. \tag{5}$$

To maintain mass conservation, the final term of the momentum equation is applied, which contains the pressure gradient:

$$\frac{\vec{V}^{n+1} - \vec{V}''}{\Delta t} = \frac{1}{\rho}\nabla P. \tag{6}$$

The pressure field is computed by evaluating the divergence of Equation (6):

$$\nabla \cdot \frac{\vec{V}^{n+1} - \vec{V}''}{\Delta t} = \frac{1}{\rho}\nabla \cdot \nabla P. \tag{7}$$

Mass conservation requires that

$$\nabla \cdot \vec{V}^{n+1} = 0. \tag{8}$$

The result is the Poisson equation:

$$\nabla P^2 = -\frac{\rho}{\Delta t}\nabla\vec{V}''. \tag{9}$$

The Poisson equation's solution allows the advancement of the solution to the new time step:

$$\vec{V}^{n+1} = \vec{V}'' - \frac{\Delta t}{\rho}\nabla P. \quad (10)$$

Since SAGE uses a uniform structured computational domain, grid metrics need not be computed, and efficient Poisson solvers using fast Fourier transform algorithms can be used. SAGE is implemented using parallel processing.

Complex geometries (i.e., a stereolithography, or STL, file that describes the solid geometry) are accommodated by using immersive boundary methods to insert the configuration in the Cartesian mesh. SAGE identifies points inside the configuration and sets the velocities at these points to zero. Grid points surrounding the surface of the geometry are assigned a value corresponding to their normal distance to the surface, with points inside the configuration being assigned a negative "distance." A distance of zero is the *level surface* corresponding to the configuration surface but is not explicitly used. The strength of the surface confinement applied is proportional to the distance function so that the flow solver interprets the level surface, where the distance function equals zero, as a solid surface. Using a conventional solver that does not use a distance function, immersing the model geometry into a coarse structured grid, would give poor results since the resulting "staircase" effect would yield an unrealistically thick viscous boundary layer. Surface confinement avoids that pitfall of the staircase effect, giving a thin, smooth boundary layer. Allowing the use of coarse, uniform structured grids and surface confinement SAGE allows insertion of geometries and terrain into the computational grid without requiring time-consuming body-fitted grid generation. This also makes it well suited to simulating changes in terrain topology (e.g., from drifting snow). The evolving surface contour can be automatically accounted for by applying a distance function to the evolving "ground" surface that changes as the simulation progresses.

2.1.2 Field and surface confinement

Field confinement helps to preserve the convecting vortical structures of the flow field without resorting to computationally expensive high-order numerical methods. In this approach, $\hat{n}$ is the normalized gradient of the vorticity magnitude,

$$\hat{n} = \frac{\nabla|\vec{\omega}|}{|\nabla|\vec{\omega}||}, \quad (11)$$

and numerically transports vorticity toward the vortex core (Wenren et al. 2006). The continuity equation is satisfied for surface and field confinement; however, the momentum equations are not explicitly satisfied. Yet, due to flows where the vortex core strength is high, momentum is almost exactly conserved with this formulation. Wenren et al. (2006) refer to this version as VC1, and we use it in the model described here. If complete conservation of momentum is required (e.g., for flows where the vortices are convected by a small external velocity), then VC2 confinement can be employed (Lynn and Steinhoff 2007).

Surface confinement is a simple boundary-layer model with $\hat{n}$ normal to the body surface (i.e., where the distance function is zero). In this case the vorticity is transported toward the surface, keeping the boundary layer thin (contained within a few grid cells).

2.2 Particle entrainment, dispersion, and deposition (PEDD)

As Ryerson et al. (2005) explained, a two-phase flow model is necessary to model the effects of particle drag and momentum. However, originally SAGE was a single-phase model and therefore not capable of simulating particle movement (Ryerson et al. 2005). Haehnel et al. (2008) coupled the flow solver with a particle transport model to allow modeling of the two-phase flow. This was a general model for predicting windblown particulates (i.e., dust, which can largely be treated as a passive scalar moving with the flow) lifted into the air from a variety of ground cover types. In this work, we incorporated enhancements into the original PED model (1) to account for differential velocity between the particles and flow (effects of fluid drag accelerating particle motion) and (2) to include particle deposition and drift formation over time scales relevant to drifting snow. The resulting model is the particle entrainment, dispersion, and deposition (PEDD) model. Sections 2.2.1–2.2.5 detail how we have incorporated these improvements into the code.

Haehnel et al. (2008) implemented a one-way coupling approach in SAGE-PEDD; that is, it models the momentum exchange from the fluid to the particles, but the effect of the particle drag on the flow is considered negligible and is ignored. This assumption is generally acceptable for dilute two-phase flows (particle concentrations less than 10% by volume). The PEDD model is integrated into SAGE through a series of sequential subroutines. First the flow field for each time step is obtained, then the particulate phase is convected based on the updated flow field.

The PEDD is made up of two parts: (1) an entrainment and deposition model that provides a source boundary condition for the particles leaving or impinging on the ground and (2) a dispersion model to simulate the convection of the particles throughout the domain. We assume the fluid flow is predominantly parallel to the packed snow surface. In this case, particles are removed from the surface due to aerodynamic lift or being knocked loose by other particles impacting the bed, a process known as saltation. Particles are then lifted up out of this saltation layer through turbulent diffusion. The transport equation of interest is the convection-diffusion equation:

$$\frac{\partial \gamma}{\partial t} + \frac{\partial u_p \gamma}{\partial x} + \frac{\partial v_p \gamma}{\partial y} + \frac{\partial \left(w_p - w_f\right)\gamma}{\partial z} =$$

$$D\left(\frac{\partial^2 \gamma}{\partial x^2} + \frac{\partial^2 \gamma}{\partial y^2} + \frac{\partial^2 \gamma}{\partial z^2}\right) - \frac{\partial}{\partial x}\overline{\gamma' u_p'} - \frac{\partial}{\partial y}\overline{\gamma' v_p'} - \frac{\partial}{\partial z}\overline{\gamma' w_p'}. \quad (12)$$

This accounts for convection and diffusion in three dimensions. The concentration, γ, varies spatially and temporally. The particle velocities in the three coordinate directions are u_p, v_p, and w_p. Gravitational effects are accounted for via the particle fall velocity, w_f. The Reynold sediment fluxes in the three directions are $\overline{\gamma' u_p'}$, $\overline{\gamma' v_p'}$, and $\overline{\gamma' w_p'}$, where the bar denotes the mean value. The entrainment or deposition of the snow is governed by

$$Q_s = \overline{\gamma' w'}|_{z=\zeta}, \quad (13)$$

which is provided as a boundary condition via a suitable "entrainment function" and where ζ is the elevation of the snow surface. We apply $\overline{\gamma' u_p'} = \overline{\gamma' v_p'} = 0$ since at the bed surface these are negligible terms in comparison to Q_s. We assume the advection terms dominate since the wind velocities, in general, are large, making the advection terms much larger than the diffusion contribution. As such, we ignore the effects of diffusion (i.e., the diffusion coefficient, $D = 0$). These assumptions greatly simplify Equation (12) so that the time-dependent change in concentration is a function of the particle velocity-concentration gradients in the three coordinate directions accompanied by an appropriate boundary flux condition, Q_s.

A key aspect of modeling entrainment and dispersion is the formulation of the boundary condition, Q_s. Numerous works have considered particle

entrainment due to flow parallel to a packed bed (Etoh and Fukushima 2001; Garcia 1989; Pomeroy and Gray 1990; Cao 1997). The equation we adopted for this work is

$$Q_{si} = \gamma_{si} U_e, \tag{14}$$

where U_e is the ejection velocity of the particle from the bed. Q_s is determined by computing a uniform concentration for the grid nodes within the saltation layer. The saltation layer concentration, γ_s, is calculated according to

$$\gamma_{si} = f_i m K \frac{(T_* - 1)}{\sqrt{T_*}} \left(\frac{A_{si}}{A_0}\right) \rho_p \frac{\rho}{\Delta\rho}, \tag{15}$$

where

f_i = the mass fraction of the ith particle class in the snowpack;
m = a factor accounting for soil moisture (m = 1 for dry soils);
K = 0.0045, a nondimensional constant;
T_* = u_*/u_{*t}, the threshold friction velocity ratio;
A_0 and A_{si} = the reference and ith particle surface area per unit mass, respectively;
ρ_p = the particle density; and
$\Delta\rho$ = $\rho_p - \rho$.

Equation (15) is a generalized model for a range of soil types that was derived from observations of Haehnel, Buck, and Song (2014). For generality, Equation (15) includes the effects of moisture on soil entrainment. Presently the effects of moisture on snow entrainment have not been adequately quantified to assess the way moisture effects for soils modeled in Equation (15) apply to snow. For simplification, we assume the snow to be dry ($m = 1$), which removes the effect of moisture from the calculation.

The final components needed for the snow-surface boundary condition are estimates of u_* and u_{*t}. The equation used for u_{*t} is based on the work of Bagnold (1941) and later built upon by Iversen and White (1982) and Shao and Lu (2020):

$$u_{*t} = A\sqrt{\frac{\Delta\rho}{\rho} g d_p + \frac{\beta}{d_p \rho}}, \tag{16}$$

with $A = 0.1109$ and $\beta = 3 \times 10^{-4}$ N/m.* To estimate the friction velocity, the flow near the surface is assumed to follow a logarithmic velocity profile:

$$U(z) = \frac{u_*}{\kappa} \ln\left(\frac{z}{z_0}\right), \tag{17}$$

where

$U(z)$ = the vector magnitude of the fluid velocity parallel to the ground plane (i.e., u and v velocity components) at height z;
κ = 0.4, the Von Karman's constant; and
z_0 = the aerodynamic roughness height of the snow surface.

Owing to flow turbulence and changes in the ground geometry as snow deposits, U is a spatially and temporally varying field. Knowing the time varying U at a reference height z, the friction velocity can be readily determined from Equation (17).

A time-accurate solution to the surface-friction velocity is required to couple SAGE to the PEDD model to define the surface boundary condition. As mentioned above, SAGE both requires a uniform, structured grid and neglects flow viscosity effects. The uniform grid is required to accurately capture the vortical structure of the flow. In practice, this makes the grid too coarse near the surface to compute surface shear stress.

To estimate the surface-friction velocity, either the correct near-bed velocity profile needs to be generated by the solver or an approximation of the velocity profile can be made. To have a uniform grid that accurately resolves the near-bed profile would require individual cells less than 2 cm square. This fine resolution puts the solution out of reach for all but massively parallel high-performance computers. Thus, the latter method is used, assuming a logarithmic velocity profile: Equation (17). The reference height and velocity used to solve for the friction velocity are obtained from the grid node immediately above the surface.

* For a full list of the spelled-out forms of the units of measure used in this document and their conversions, please refer to *US Government Publishing Office Style Manual*, 31st ed. (Washington, DC: US Government Publishing Office, 2016), 245–252, https://www.govinfo.gov/content/pkg/GPO-STYLEMANUAL-2016/pdf/GPO-STYLEMANUAL-2016.pdf.

2.2.1 Snow depth

Equation (15) is solved using Equations (16) and (17) at each time step in each grid cell adjacent to the ground or evolving snow surface. This gives the airborne snow concentration resulting from the fluid shear stress acting on the snow surface. The solution is then advanced to compute the volume of snow moved (advected) into and out of each grid cell. The resulting change in concentration at the snow surface is then converted into a change in snow volume, ΔV_s:

$$\Delta V_s = \frac{V_{cell}\Delta\gamma}{\rho_s}, \tag{18}$$

where $V_{cell} = \Delta x \Delta y \Delta z$, the volume of the grid cell, and ρ_s is the bulk density of the snow on the ground. The snow volume on the left-hand side of Equation (18) can be expressed as the horizontal area of the grid cell multiplied by the change in snow depth, $\Delta\zeta$. What remains is the equation for the change in snow depth as a function of the change in concentration:

$$\Delta\zeta = \frac{\Delta z\Delta\gamma}{\rho_s}, \tag{19}$$

where Δz is the grid size in the z direction. Positive $\Delta\gamma$ indicates a surplus of snow in the grid cell and results in deposition. Conversely, negative values of $\Delta\gamma$ will erode the snow surface, provided that there is snow to erode (i.e., snow depth, $\zeta > 0$).

2.2.2 Scaling time

The numerical time step for a simulation depends on the numerical solution scheme implemented in the flow solver. SAGE-PEDD uses an explicit numerical method, and the time-step size is limited. For this work, the maximum stable numerical time step, *dt*, needed to run the simulations is the time within which the snow particles move a distance two-tenths of the computational grid cell size. For example, for one case we considered where the grid cell size was 4 ft (1.2 m) and the maximum wind speed was 52 ft/s (16 m/s), *dt* equaled 0.01538 s. The duration of a winter season for this example was 222 days (15 February–15 October), hence the number of time steps to do an entire simulation was over 1.2 billion. It took approximately 1723.4 compute seconds per time step (using 704 CPUs, that is 2.45 s of wall-clock time per time step). To do a full simulation of one winter season without any adjustments for scaling time, it would take about

93 years to simulate on the current US Army Engineer Research and Development Center's Onyx high-performance computing system. To make the run time for these cases reasonable, we implemented the following adjustment to scale time.

We introduced a snow-density scaling factor, ρ_{sc}, a nondimensional value that is used to augment the snow depth for each computational time step (or computational iteration). The increment in snow, $\Delta\zeta$, added to the existing snow surface in a grid cell adjacent to the ground at each time step is

$$\Delta\zeta = \rho_{sc}\frac{\Delta z \Delta \gamma}{\rho_s}. \tag{20}$$

When ρ_{sc} equals 1, the deposition depth is not augmented, and the depth of snow deposited for each iteration is determined by the bulk density of the snowdrift (i.e., the concentration of new suspended snow is compacted to a density equal to the bulk density of the snow). We consider a ρ_{sc} equal to 1 a tight coupling between the flow field and the snow deposition rate. Because the computational time steps are small (order of 1/100 s or smaller), the changes in concentration are small, and the changes in snow depth are small for each iteration. We use the factor ρ_{sc} to loosen the coupling between the flow field and snowdrift evolution. ρ_{sc} greater than 1 allows the amount of snow deposited to be larger for each computational iteration than changes driven by the simulated flow field would dictate, thereby reducing computation time.

The assumption is that amplifying the deposited snow depth by a factor of 10 or 100 will only increase the depth of the snow from around 0.1 mm per time step to 1 to 10 mm per time step. This small increase in snow depth does not depart significantly from the near-term trend that the drift will take as the simulation progresses or have a gross effect on the flow field; therefore, the flow can be loosely coupled to changes in the deposited drift shape. However, the factor ρ_{sc} cannot be too large or the snowdrifts grow too rapidly for changes in the flow field to stably respond (i.e., the coupling would not be tight enough). Yet, if ρ_{sc} is very small, the simulation takes months or years to complete. We have found that this approach is a work in progress and that the level of coupling, therefore the value of ρ_{sc}, needs to be adjusted based on computational grid characteristics (e.g., grid resolution and domain size). At present, for accurate time scaling, calibration of ρ_{sc} to validation data (e.g., snow survey data) gives the most accurate results. Despite the additional time needed for model calibration, this

generally is a small price to pay compared to the overall savings in computation time.

2.2.3 Domain boundary conditions

In general, we applied outlet boundary conditions at the far field (top and sides of the computational domain). However, if a crosswind or headwind is imposed, inlet boundary conditions are applied at the appropriate sides of the domain. A no-slip boundary condition is applied at the ground surface. The inlet velocity varies with height above the snow surface according to Equation (17), using $U(z)$ as the specified inflow freestream velocity, V_∞, specified at the reference height of 10 m. V_∞can be specified as a fixed value for the duration of the simulation or specified by an external text file, such as observed meteorological data, to give a time-varying flow field.

Another element in defining the inlet boundary condition is the formulation of the snow-concentration profile. Initializing the concentration profile allows for a smaller computational domain by reducing the upwind extents that would be required if the concentration profile were to evolve solely within the computational domain as a result of flow-induced particle entrainment and dispersion into the flow. To address this, we used measured concentration data from Budd, Dingle, and Radok (1965) to create an empirical expression for the concentration profile based on the values of the input velocity V_∞. Figure 1 shows the concentration data plotted for wind speeds varying from 38.4 to 72.5 ft/s (11.7 to 22.1 m/s). We explored numerous forms for the concentration equation, including the expression given by Beyers and Waechter (2008), which we found to underpredict the observed measurements. The form adopted for our work follows the simple form:

$$\gamma(z) = \frac{A}{z}, \tag{21}$$

where A is a fitting parameter. Figure 2 plots empirically determined values of A against wind speed.

Figure 1. Concentration profile measurements for varying wind speeds. Dotted lines indicate fitted curves.

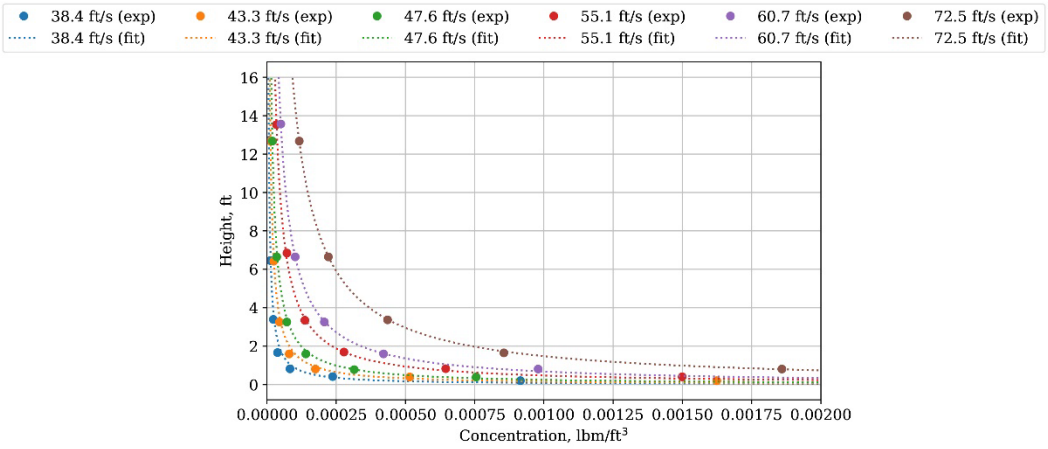

Figure 2. Plot of fitting parameter, *A*, versus wind speed.

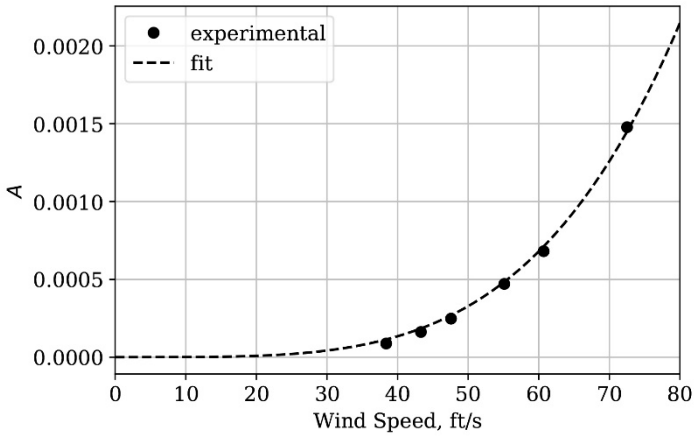

The trend is described by

$$A(V_\infty) = B|V_\infty^4|. \tag{22}$$

The constant B has a value of 5.244×10^{-11} lbm/ft² (2.566×10^{-10} kg/m²) for V_∞ in feet per second and γ in pound mass per cubic feet. The results of Equations (21) and (22) are combined to yield

$$\gamma(V_\infty, z) = B\frac{|V_\infty^4|}{z}, \tag{23}$$

where z is the distance above the snow surface at the inlet. The simplicity of this formulation leads to nonphysical high values of concentration when z is very small. To remedy this, when the inlet concentration near the ground—$\gamma(V_\infty, 0)$, computed using Equation (23)—is greater than that

computed by Equation (15) at the inlet, $\gamma_s|_{inlet}$, we set $\gamma(V_\infty, 0)$ equal to $\gamma_s|_{inlet}$.

2.2.4 Particle drag effects

Effects of drag on particle motion can influence the rate and location of deposition. The default configuration does not account for drag effects (i.e., particles are treated as flow-following passive scalars with gravitational effects included), resulting in faster run times. However, the SAGE-PEDD includes an optional model to account for a differential velocity between the fluid and particles and the effects of fluid drag on particle acceleration. The acceleration of the particles, $a_d = (dU/dt)_d$, due to drag can be readily calculated from Newton's second law, $a = F/m$, where F is the drag force, a function of the drag coefficient, C_D, which depends on the particle shape and Reynolds number. Because generally the relative velocity between the fluid and particle, U_{rel}, is small, C_D can be computed assuming Stokes flow. Thus, the acceleration can be calculated by

$$\left(\frac{dU}{dt}\right)_d = \frac{3}{4}\frac{C_d U_{rel}^2}{\rho_p d_p}, \tag{24}$$

where ρ_p is the particle density and d_p is the particle diameter.

2.2.5 Snow aging/sintering

Proper, long-term characterization of the snowpack must account for changes in snow density and strength, which influence the threshold friction velocity over time. Snow may begin to coalesce or sinter into a harder, denser layer as soon as it is deposited. Liston et al. (2007) provide a framework to model the rate and spatial distribution of snow hardening. Liston et al.(2007) assume that snow strength, and therefore u_{*t}, is solely a function of bulk snow density on the ground. The snowpack is approximated using a two-layer model composed of a movable, soft snow layer and an immovable, hard snow layer. Figure 3 outlines the decision process for updating the bulk density, ρ_s, of the soft snow layer.

Figure 3. Flow chart detailing the snow-hardening decision tree, where $\Delta\zeta/\Delta t$ is the change in snow depth for the current time step, u_{10} is the wind speed at a reference height of 10 m, and $u_{*t,max}$ is the maximum friction velocity generated by naturally occurring winds (generally, $u_{*t,max}$ = 1.7 m/s, corresponding to u_{10} = 40 m/s).

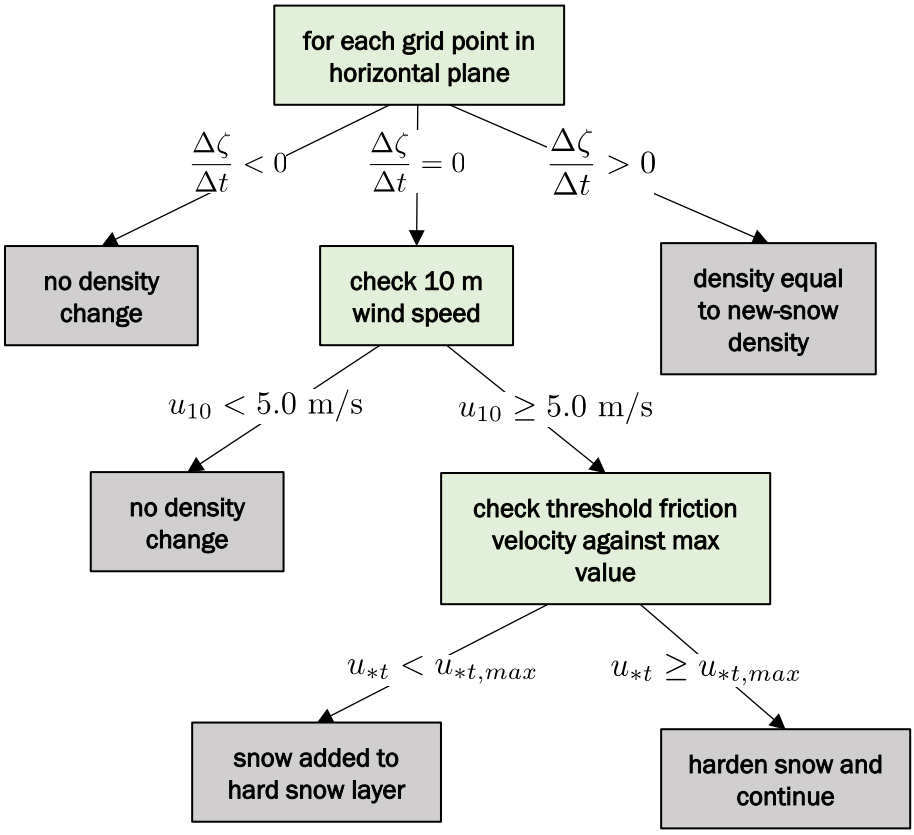

The user defines the new snow bulk density, ρ_{ns}. Values of 275–350 kg/m^3 are typically used in SAGE-PEDD. During periods of local inactivity (i.e., $d\zeta/dt = 0$ for a given location in the grid) and wind speeds equal to or exceeding 5 m/s, the density of the snow increases according to the equation

$$\frac{\partial \rho_s}{\partial t} = CA_1 H \rho_s \exp\left[-B\left(T_f - T_s\right)\right]\exp[-A_2\rho_s], \tag{25}$$

where T_f and T_s are the freezing and snow-surface temperatures, respectively; A_1, A_2, and B are empirical constants equal to 0.00013 m^{-1}, 0.021 m^3/kg, and 0.08 K^{-1}, respectively; and C equals 0.10, a nondimensional constant that controls the simulated rate of change of the snow density. The wind-speed contribution for speeds greater than 5 m/s is given by H as

$$H = E_1 + E_2\left(1 - \exp\left(-E_3\left(\frac{1}{\kappa}\ln\left(\frac{2}{z_0}\right)\left(u_* - u_{*t,fresh}\right)\right)\right)\right), \quad (26)$$

where $u_{*t,fresh}$ is the threshold friction velocity for fresh snow, and E_1, E_2, and E_3 are additional empirical constants equal to 5.0 m/s, 15.0 m/s, and 0.2 m/s, respectively.

Snow density is related to strength using the uniaxial compression measurements of Abele and Gow (1975). A curve Liston et al. (2007) fitted to the data indicates that the snow hardness, σ, varies according to

$$\sigma = 1.36\exp(0.013\rho_s), \quad (27)$$

where σ is in kilopascals and ρ_s is in kilograms per cubic meter. Next, the snow hardness is related to the threshold friction velocity, u_{*t}, according to data from Kotlyakov (1961). For snow densities of 300–450 kg/m^3,

$$\sigma = 267u_{*t}. \quad (28)$$

Similar expressions can be derived for snow densities of 50-300 kg/m^3 as is done for Equations (27) and (28). Combining Equations (27) and (28), and similar equations for densities in the range of 50–300 kg/m^3, yields

$$u_{*t} = \begin{cases} 0.010\exp(0.003\rho_s), & 50 \le \rho_s \le 300 \\ 0.005\exp(0.013\rho_s), & 300 \le \rho_s \le 450 \end{cases}. \quad (29)$$

Note Liston et al. (2007) assume that when ρ_s exceeds 450 kg/m^3, the snow transitions to the hard snow layer, which is immovable for all future time steps. This model is used to capture the effects of natural snow sintering on inhibiting snow entrainment. New snow deposited on top of the hard snow layer forms a new soft snow layer.

3 Summary and future work

In this effort, we extended the capability of our previous work, SAGE-PED, a two-phase computer code. SAGE-PED was developed to model particle entrainment and dispersion (PED) for assessing the effects of suspended particles on degraded visibility. In this new effort, we have added the ability to model particle deposition, with a particular application to simulating snowdrift evolution surrounding buildings. The new code is called SAGE-PEDD (particle entrainment, dispersion, and deposition).

This document outlined the theory applied in the new model. In addition to considering deposition, we have added several new features needed to completely and efficiently model snowdrift evolution. These include appropriate particulate inflow conditions at the computational domain boundaries, the ability to account for snow aging (or sintering) that hardens the snow over time, and meteorological data as inflow conditions to drive the simulation. Currently, the model considers varying inflow wind speed. Updating the model to appropriately handle varying wind direction is a future work.

We have introduced a novel approach in the model to speed up the computation where the snowdrift evolution can be loosely coupled to the computational time step and time-dependent flow field. We accomplished this by augmenting the deposited snow at each time step via a density scaling factor. We have found this scaling factor is dependent on the resolution and extents of the computational grid, and possibly other factors. Currently, to accurately scale the time in the simulation this density scaling factor needs to be calibrated to field data. Future work will address how to determine the density scaling factor without the need for model calibration.

Overall, our new SAGE-PEDD model allows accurate and computationally efficient simulation of snowdrift evolution around buildings. This model can give insight into the effects of building design on snowdrift location and depth and in turn can be used to design buildings that minimize the impacts of snowdrifts on daily and seasonal operations, saving the US Government organizations time and resources.

References

Abele, G., and A. J. Gow. 1975. *Compressibility Characteristics of Undisturbed Snow*. Research Report 336. Hanover, NH: US Army Cold Regions Research and Engineering Laboratory. https://apps.dtic.mil/sti/pdfs/ADA012113.pdf.

Bagnold, R. A. 1941. *The Physics of Blown Sand and Desert Dunes*. London: Methuen.

Beyers, J. H. M., and B. Waechter. 2008. "Modeling Transient Snowdrift Development around Complex Three-Dimensional Structures." *Journal of Wind Engineering and Industrial Aerodynamics* 96 (10–11): 1603–1615. https://doi.org/doi:10.1016/j.jweia.2008.02.032.

Budd, W., R. Dingle, and U. Radok. 1965. "The Byrd Snowdrift Project: Outline of Basic Results." In *Studies in Antarctic Meteorology*, 71–134. American Geophysical Union.

Cao, Z. 1997. "Turbulent Bursting-Based Sediment Entrainment Function." *Journal of Hydraulic Engineering* 123 (3): 233–236. https://doi.org/10.1061/(ASCE)0733-9429(1997)123:3(233).

Etoh, T., and Y. Fukushima. 2001. "Numerical Analysis of Turbidity Currents Using K-ε Turbulence Model." In *Proceedings of the 8th International Symposium on Flow Modeling and Turbulence Measurements*, 4–6 December, Tokyo, Japan.

Garcia, M. H. 1989. "Depositing and Eroding Sediment-Driven Flows: Turbidity Currents." PhD Thesis, University of Minnesota.

Haehnel, R., M. Moulton, Y. Wenren, and J. Steinhoff. 2008. "A Model to Simulate Rotorcraft-Induced Brownout." In *Proceedings of the American Helicopter Society 64th Annual Forum*, 29 April–1 May, Montreal, Canada.

Haehnel, R., N. Buck, and A. Song. 2014. "Moisture Effects on Eolian Particle Entrainment." *Journal of Environmental Fluid Mechanics* 14 (1): 135–156. https://doi.org/10.1007/s10652-013-9299-y.

Iversen, J. D., and B. R. White. 1982. "Saltation Threshold on Earth, Mars and Venus." *Sedimentology* 29:111–119. https://doi.org/10.1111/j.1365-3091.1982.tb01713.x.

Kotlyakov, V. M. 1961. "Results of a Study of the Processes of Formation and Structure of the Upper Layer of the Ice Sheet in Eastern Antarctica." *Antarctic Glaciology* 55:88–99.

Liston, G., R. Haehnel, M. Sturm, C. Hiemstra, S. Berezovskaya, and R. Tabler. 2007. "Instruments and Methods Simulating Complex Snow Distributions in Windy Environments Using SnowTran-3D." *Journal of Glaciology* 53 (181): 241–256. https://doi.org/10.3189/172756507782202865.

Lynn, N. F., and J. Steinhoff. 2007. "Large Reynolds Number Turbulence Modeling with Vorticity Confinement." In *Proceedings of the 18th AIAA Computational Fluid Dynamics Conference*, 25–28 June 2007, Miami, FL, 639–652. https://doi.org/10.2514/6.2007-3965.

Pomeroy, G. W., and D. M. Gray. 1990. "Saltation of Snow." *Water Resources Research* 27 (7): 1583–1594. https://doi.org/10.1029/WR026i007p01583.

Ryerson, C. C., R. B. Haehnel, G. G. Koenig, and M. M. Moulton. 2005. "Visibility Enhancement in Rotorwash Clouds." In *Proceedings of the 43rd AIAA Aerospace Sciences Meeting and Exhibit*, 10–13 January, Reno, NV. https://doi.org/10.2514/6.2005-263.

Shao, Y., and H. Lu. 2000. "A Simple Expression for Wind Erosion Threshold Friction Velocity." *Journal of Geophysical Research* 105 (22): 437–443. https://doi.org/10.1029/2000JD900304.

Steinhoff, J., and Y. Wenren. 2006. "An Efficient Vorticity Confinement Based Lifting Surface Method for Rotor Wake Computations." In *Proceedings of the 32nd European Rotorcraft Forum*, 12–14 September, Maastricht, The Netherlands.

Wenren, Y., J. Steinhoff, and F. Caradonna. 2005. "Application of Vorticity Confinement to Rotorcraft Flows." In *Proceedings of the 31st European Rotorcraft Forum*, 13–15 September, Florence, Italy.

Wenren, Y., J. Walter, M. Fan, and J. Steinhoff. 2006. "Vorticity Confinement and Advanced Rendering to Compute and Visualize Complex Flows." In *Proceedings of the 44th AIAA Aerospace Sciences Meeting and Exhibit*, 9–12 January, Reno, Nevada. https://doi.org/10.2514/6.2006-945.

REPORT DOCUMENTATION PAGE

Form Approved
OMB No. 0704-0188

1. REPORT DATE (DD-MM-YYYY)	2. REPORT TYPE	3. DATES COVERED (From - To)
August 2022	Technical Report / Final	FY19–FY22

4. TITLE AND SUBTITLE
SAGE-PEDD Theory Manual: Modeling Windblown Snow Deposition around Buildings

5a. CONTRACT NUMBER

5b. GRANT NUMBER

5c. PROGRAM ELEMENT

6. AUTHOR(S)
Robert B. Haehnel, Yonghu Wenren, and Luke D. Allen

5d. PROJECT NUMBER

5e. TASK NUMBER

5f. WORK UNIT NUMBER

7. PERFORMING ORGANIZATION NAME(S) AND ADDRESS(ES)
US Army Engineer Research and Development Center (ERDC)
Cold Regions Research and Engineering Laboratory (CRREL)
72 Lyme Road
Hanover, NH 03755-1290

8. PERFORMING ORGANIZATION REPORT NUMBER
ERDC/CRREL TR-22-8

9. SPONSORING / MONITORING AGENCY NAME(S) AND ADDRESS(ES)
National Science Foundation
Office of Polar Programs
Antarctic Infrastructure and Logistics
2415 Eisenhower Avenue
Alexandria, VA 22314

10. SPONSOR/MONITOR'S ACRONYM(S)
NSF

11. SPONSOR/MONITOR'S REPORT NUMBER(S)

12. DISTRIBUTION / AVAILABILITY STATEMENT
Approved for public release; distribution is unlimited.

13. SUPPLEMENTARY NOTES
Funded under Engineering for Polar Operations, Logistics, and Research (EPOLAR), ANT-21-54, "Impact of Lifting the Elevated South Pole Station on Snow Drift Accumulation on Nearby Facilities"

14. ABSTRACT
Numerical modeling of snowdrifting is a useful tool for assessing the impact of building design on operations and facility maintenance. Here we outline the theory for the SAGE-PEDD snowdrift model that has application for determining snowdrift accumulation around buildings. This model uses the SAGE computational fluid dynamics code to determine the flow field in the computational domain. A particle entrainment, dispersion, and deposition (PEDD) model is coupled to SAGE to simulate the movement and deposition of the snow within the computational domain. The report also outlines areas of future development that upgrades to the SAGE-PEDD model should address.

15. SUBJECT TERMS
Buildings--Cold regions, EPOLAR, NSF, Structural design, Snow, Snow loads, Wind-snow interaction--Computer simulation

16. SECURITY CLASSIFICATION OF:			17. LIMITATION OF ABSTRACT	18. NUMBER OF PAGES	19a. NAME OF RESPONSIBLE PERSON
a. REPORT	b. ABSTRACT	c. THIS PAGE			19b. TELEPHONE NUMBER (include area code)
Unclassified	Unclassified	Unclassified	SAR	27	